

A global methodology for 3D multi-material Laser Powder Bed Fusion processes

José Pires^{a,b}, Paulo Pinto^{a,b}, Flávio Bartolomeu^{a,b}, Filipe Silva^{a,b}, Óscar Carvalho^{a,b,*}

^a*Centre for Micro Electrical Mechanical Systems (CMEMS), Azurém, 4800–058 Guimarães, Portugal*

^b*bLABELS — Associate Laboratory, Braga/Guimarães, Portugal*

Abstract

Laser Powder Bed Fusion (LPBF) processes emerge as one of the most feasible and flexible Additive Manufacturing (AM) technologies of metallic and composites parts, as they enable the layer-wise production of complex-shaped, functionally graded or custom-tailored parts by material deposition and subsequent or simultaneous melting via a focused laser beam. Furthermore, LPBF processes also enable the fabrication of multi-material parts, highly desirable for enhancing even further the performance of such parts, by varying compositions or type within layers, unachievable by conventional manufacturing processes. However, most current commercially available systems are mono-material only, which could be partially explained by the added complexity of the multi-material processing to an already complex multi-physics problem. The trend is for the problem to get worse, as the techniques to solve it will become increasingly complex. Still, the reported methodologies seem to address only specific parts of the problem, disregarding the ‘whole picture’ scenario. In the present work, a global methodology for tackling the complexity of LPBF processes is proposed, demonstrating the added benefits for all the agents in the manufacturing chain. The design of this methodology will be discussed in detail with special focus in its core principles and tools. The methodology is then applied specifically

*Corresponding author

Email address: oscar.carvalho@dem.uminho.pt (Óscar Carvalho)

to LPBF process, adding the multi-material aspect in all directions, yielding a novel 3D Multi-Material Laser Powder Bed Fusion (3DMMLPBF) process. As a result, a simplified workflow — CAD to 3DMMLBPF-PART — is established. The software toolchain was derived from the workflow, comprising the slicer and path generator, post-processor and printer, and the post-manufacturer. A low-budget, highly customizable 3DMMLPBF equipment was built as a proof-of-concept. The workflow and associated toolchain, and the equipment were tested and validated.

Keywords: methodology, multi-material, powder bed fusion, equipment

Acronyms

3DMMLPBF 3D Multi-Material Laser Powder Bed Fusion

AI Artificial Intelligence

AM Additive Manufacturing

ASTM American Society for Testing and Materials

CAD Computer-Aided Design

CAE Computer-Aided Engineering

CAM Computer-Aided Manufacturing

CNC Computer Numerical Control

DED Direct Energy Deposition

DLD Direct Laser Deposition

DOE Design Of Experiments

EBM Electron Beam Melting

FDM Fused Deposition Material

FGM Functionally Graded Material

GUI Graphical User Interface

LMD Laser Metal Deposition

LOM Laminated Object Manufacturing

LPBF Laser Powder Bed Fusion

MMAM Multi-Material Additive Manufacturing

MMFGM Multi-Material Functionally Graded Material

NC Numerical Control

PBF Powder Bed Fusion

SEM Scanning Electron microscope

SLM Selective Laser Melting

SLS Selective Laser Sintering

STL Standard Tessellation Language

SVG Scalable Vector Graphics

UAV Unmanned Aerial Vehicles

UML Unified Modeling Language

XML eXtensible Markup Language

1. Introduction

AM is revolutionizing the way we manufacture products by providing the designer the freedom to bring the conceptualized ideas to life from ground-up, contrarily to the traditional (subtractive) manufacturing techniques which impose a pre-shape. With this theoretically ‘unlimited’ freedom comes a greater responsibility, and aid should be provided to the designer in the form of guidelines and design criteria, as a means to unlock AM full potential: as material is only added where is functionally needed, waste is minimized and the overall properties of the component being built are enhanced [1].

This idea meets its pinnacle with the concept of an Multi-Material Functionally Graded Material (MMFGM) — multi material components with materials gradations in between. The great interest on using MMFGMs is the possibility of controlling composition or structure and thus obtain components with desired local properties, as regarding mechanical, tribological, thermal properties, and others [2].

However, most current commercially available systems have been designed for mono-material part fabrication [3] and are unprepared for multi-material processing due to the lack of flexibility and processing capability. In the field of metallic and composite components the panorama is worst due to: the complexity of the multi-physics problem associated with the process used — for example, LPBF processes — which exhibit multiple modes of heat and mass transfer [4, 5, 6, 7, 8, 9] and in some instances chemical reactions [10, 11]; the vast number of process parameters [12]; and the lack of a global infrastructure that supports the development of the multi-material processes in this field, as the solutions are from proprietary nature, and therefore closed-environment, hindering the technological advances in the area.

Thus, a global methodology for the fabrication of multi-material metallic and composite parts is required to handle the inherent complexity and leverage the process’s knowledge, providing an AM process database — as suggested by Gu et al. [13] — to all key agents in the manufacturing chain.

2. Reviews

2.1. Additive Manufacturing

The fundamental premise of AM is quite simple: adding and bonding the material(s) to create the part only where it is/are needed, typically in a layer-by-layer fashion via Computer Numerical Control (CNC) displacement, from imported three-dimensional (3D) model data [14]. The 3D part is ‘assembled’ by bonding materials, either like or dissimilar, with each new layer of material being a manifestation of the 3D model cross-sectional data. These models are typically in the Computer-Aided Design (CAD) form in Standard Tessellation Language (STL) file format and are numerically sliced into many fictitious layers/cross-sectional data from which the manufacturing paths can be generated, dictating the CNC displacement. A wide variety of AM application have been reported namely: Unmanned Aerial Vehicless (UAVs) [15], fuel nozzles [16], houses [17], tooling [18, 19], biomedical implants [20], among others.

To accomplish the effective material bonding, the successful combination of material and energy delivery is required, differing with the material and the AM process[14, 21]. The AM processes can be classified by [22]:

- *state of raw material:* liquid, solid sheet or discrete particle;
- *type of material:* metal (layer or direct deposition); polymer (Fused Deposition Material (FDM), stereolithography, polyjet); paper (Laminated Object Manufacturing (LOM); wood (stratoconception).

Sometimes, terminology will differ but American Society for Testing and Materials (ASTM) in attempt to standardize this classification recognizes the following AM methods [14]: material extrusion, material jetting, sheet lamination, vat polymerisation, binder jetting, Direct Energy Deposition (DED) and Powder Bed Fusion (PBF).

The AM process is traditionally ‘open-loop’ due to its lower complexity and lower cost; however feedback control is being introduced to ensure better part quality, in some cases with real-time characteristics [23, 24].

60 *2.2. Laser-based Additive Manufacturing*

When it comes to the additive manufacturing of metallic parts and composites DED and PBF are the most proven and feasible methods [14, 25]. Both processes involve the deposition of powder metal (or less common preforms such as wire) and their simultaneous or subsequent melting, respectively, via a focused thermal energy source, namely an electron beam or a laser beam. In case a laser beam is used the processes can be referred as form of LPBF, while DED can be further specified as Direct Laser Deposition (DLD) [14]. The usage of an electron beam (Electron Beam Melting (EBM)) makes high scanning speed possible (up to several km/s) due to the lack of moving parts to guide the building spot [22]; however, the increased complexity and cost does not make it commercially viable yet. As a result, LPBF processes are the current bet for commercial and industrial applications.

70 *2.3. Multi-Material Additive Manufacturing*

The capability to fabricate multiple material parts is highly desirable as it allows for the accurate placement of material according to its functionality, providing custom-tailored parts for specific applications with enhancement of its mechanical properties and behaviour in service. However, most current commercially available systems have been designed for mono-material part fabrication [3]. The emerging Multi-Material Additive Manufacturing (MMAM) technology can enhance the AM parts performance by varying compositions or type within layers, unachievable by conventional manufacturing processes [25], without the need for complex manufacturing process and expensive tooling [26, 27].

80 The range of applications are vast and pivotal. In the biomedical engineering field, MMAM enabled the production of 3D engineered tissue (3D spinal cord [28]), biomedical devices such as microneedle arrays [29] and diagnostic devices [30], multi-material cellular structures targeting orthopedic implants [31], and 3D artificial models for preclinical or preoperative surgical training [32, 33], among others. In the soft robotics field, where flexibility is key for complex actuations and motions, MMAM enabled the production of pneumatic driven

90 elastomeric actuators [34] and direct integration of functional components required for it (e.g., a silver-nanoparticle ink acting as a resistive heating element [35]). In electronics MMAM is critical for direct manufacturing of 3D electronic devices where electrically dissimilar materials including conductors, semiconductors, and dielectrics are integrated together [26]. Some examples are
95 a 3D magnetic sensor with integrated electronics components and conductive paths [36], stretchable strain or pressure sensors [37] and a highly stretchable electronic LED board [38], yielding high potential for wearable electronics, and even a fully 3D printed and package Li-ion battery [39].

To achieve this superior performance over AM, different materials or chemicals need to be physically delivered to any point in the 3D space during the additive manufacturing. In some processes, like direct 3D printing in Objet, FDM, this is relatively straight-forward to achieve as the materials are deposited in the platform dot-by-dot or line-by-line via nozzles; to incorporate multi-material fabrication multiple nozzles can be added [25].

105 For multi-material fabrication of metals, a similar result could be achieved through the use of LENS process or DLD, as they can use multiple nozzles/hoppers in the part fabrication. For example, multi-material components manufactured by Laser Metal Deposition (LMD) has been demonstrated in literature [40, 41]. However, in other processes, like Selective Laser Sintering (SLS),
110 Selective Laser Melting (SLM), LOM, this is not trivial, as the materials are delivered as whole layer by a scraper or as a solid sheet, requiring new material delivery systems to be first developed [25]. Nonetheless, SLM provides higher precision, smaller feature size and the ability to produce lightweight structures based on lattices, which are appealing features for turbine blades that cannot be
115 easily achieved by LMD [42, 43]. On top of that, DLD is a more difficult process to master due to added complexity of deposition control, on top of the melt-pool control, which can cause variations in the laser spot due to local increase of part's height as a result of the deposition [44].

Focusing on the SLM process, the key process parameters are laser power,
120 scanning speed, layer thickness and hatch spacing [45]. Recent works demon-

strated its feasibility for multi-material manufacturing, by using modified industrial machines or self-developed prototypes, but with material variation obtained layerwise only. Using a modified industrial machine, C18400 copper have been successfully deposited on top of 316L stainless steel and AlSi10Mg [46, 47]. However, there is no control of the transition zone between the two materials, which is the most critical in a multi-material part. As aforementioned the powder delivery system is critical for the multi-material fabrication using SLM and must be carefully designed to prevent cross-contamination between materials, thus, special focus was given to it. Demir and Previtali developed a double hopper powder delivery system based on piezoelectric transducers which enabled the manufacturing of a Fe/Al-12Si specimen, with an intermixed region between the two materials [48]. Kumar et al. used glass pipettes as ‘hopper-nozzles’ to spread powder, by means of gas pressure or vibration feed, allowing a precise powder delivery, without the need to vacuuming the excess [49]. Another approach towards a graded transition is the use of selective recoaters combined with a special processing scheme for powder removal, where one material is selectively deposited, then melted before the other one is delivered, and finally excess powder is vacuumed [50, 51, 52]. Anstaett et al. proposed an SLM system capable of depositing two different powders, combining a Cu-alloy and a tool steel to produce a multi-material component [53].

On the commercial field, Admatec developed an industrial SLM machine which spreads the raw material as a slurry, thus allowing to combine multiple materials [54]. By heating the feedstock the binder eventually evaporates and the metal powder can be successively processed.

Very recently, Walker et al. [55] developed a LPBF machine technology for graded alloy processing, with the capability to deposit location specific powder of varying material composition in any 3-dimensional location, thanks to multiple powder hoppers. The Open Additive Open Machine Control TM (OMC) software is used (proprietary source) to control all process operations, namely, powder deposition, control of the vacuum nozzle, and application of location specific processing parameters. Furthermore, the composition mixtures are cre-

ated prior to processing and separated into individual hoppers or the powder supply, for multi-material processing, but no design guidelines are provided for the common user: how to design a multi-material part that the machine is able
155 to produce, with the required functionality?

Thus, in the first iteration of the methodology proposed SLM process will be considered, contingent of the need for a better powder delivery system.

2.4. Methodologies

Some methodologies for multi-material processing have been proposed in the
160 literature [56, 57, 52]. Chiu et al. [56] proposed a methodology for direct digital manufacturing of 3D Functionally Graded Material (FGM) objects via 3D printing based on the geometrical — 3D CAD model — and material information — color property. The resultant colors are determined by Computer-Aided Engineering (CAE) analysis results which convert the design criteria (strength)
165 requirements, binder concentration requirements, primary binder requirements using 3D pixels — voxels. The design of the FGM model then becomes the problem of determining the average binder concentration applied to each pixel of the model. It also reports the problems of the current FGM model representation using plain STL files as it only conveys geometrical information and
170 reviews some alternatives like material tree structure [58], ‘grading source’ representation [59], vector valued function spanning a material space [60], STEP + data planning model [61], among others. However, this methodology is limited to direct deposition technologies and the range of change of the binder concentration is narrow.

175 Ponche et al. [57] proposed a new methodology of design for AM applied to LPBF processes, organized into three main steps — part orientation, functional optimisation and manufacturing paths optimisation — that takes into account the geometrical deviations induced by the physical phenomena occurring during the process as means to produce more accurate and reliable parts. However, it
180 is only suited for DLD process, it uses a considerable amount of different tools (Morfeo, Topostruct, MATLAB) and it uses empirical manufacturing rules.

Chivel [52] proposed a new approach to multi-material processing in SLM introducing a new SLM machine concept with improved build platform cleaning and optical systems, including a monitoring system with a high speed digital
185 CCD camera and pyrometer for melt-pool control. The multi-material fabrication was conducted through a clever cleaning and powder recovery system design via granulometric sieving (according to particle diameter) and alternate descent and ascent of the printing bed to remove the powder. To avoid wash out of solid-melt interface, a special strategy of scanning was proposed to reduce
190 the time of solid-melt contact, consisting of a spiral scanning path carried out from the centre to the periphery. However, the alternate descent and ascent of the printing bed seems to be unnecessary, which suggests improvements can be made, and the machine is patent-protected which inhibits any modification, hindering the customisation requirement of the manufacturing process.

195 The proposed methodology in the present work borrows some concepts from the preceding methodologies, aiming to fill the gaps left by them through a global perspective over LPBF processes, leveraging the process's knowledge throughout the manufacturing chain.

3. LPBF methodology

200 3.1. Motivation

The proposed methodology arises mainly from three important aspects: the lack of a methodology that encompasses the LPBF process as a whole, considering the key agents and leveraging the overall existing knowledge; the need to build an equipment to fabricate MMFGMs, as the currently available processing
205 technology does not fit the desired customization and freedom requirements; the inherent complexity of LPBF processes, even for a single material, and, since the trend is for the complexity to increase as we enter the field of multiple materials and FGMs, an efficient way to handle the complexity is required.

Furthermore, the current commercial equipments are expensive and not very
210 customizable, undermining the machine's full potential, as the end-user has

limited access to the machine and process parameters. This is especially critical in the research environment, diminishing the research opportunities, increasing inequalities in the field, and, most important of all, hindering the evolution of the LPBF processes.

²¹⁵ The underlying philosophy follows, in a sense, the open-source one, as transparency is undoubtedly a desirable feature, enabling the convenient scrutiny of all stages of the process, which is a science's premise. This holds valid for both software and hardware tools.

3.2. Core Principles

²²⁰ Knowledge, the theoretical or practical understanding of a subject, is the most important human asset. However, knowledge acquisition is a nonlinear process, as a single piece of additional data can invalidate complete models [62]. Still, LPBF knowledge is scattered around its agents without an apparent connection. Moreover, some employed techniques in LPBF processes are empirical-based ²²⁵ [14], which obviously requires the capture of the context and the rationale behind these decisions. The key idea here is to capture the knowledge and the associated context and delivery it to the appropriate handler, leveraging its efficient usage in favour of the overall process.

The core principles of the methodology are:

- ²³⁰ • *Abstraction*: layer(s) to abstract from the internal specifics of the process should be provided by means of tractable interfaces;
- *Modularity*: every component of the process should be replaceable by another of identical functionality;
- *Independence*: the process should be agnostic about the inputs, as long as the valid interfaces are respected;
- ²³⁵ • *Flexibility*: capable of handling different inputs/components as new parameters or the conjunction of its effects can be used in the process; it should support different materials, machines modules, slicing strategies, etc.;

- ²⁴⁰ • *Extensibility*: new components should be added without compromising the process;
- *High customization*: both software and hardware based components should allow a high customization of its operation;
- *Capability of managing the different information flows*: pre-process, process and post-process data should be collected and delivered to its handler in a convenient way;
- ²⁴⁵ • *Evolution*: The acquired knowledge should be used for improvement of the process;
- *Guidance to end-users*: the acquired knowledge should enable the creation of guidelines and heuristics to aid the end-user;
- ²⁵⁰ • *Maximization of process's control*: an open developing environment enhances end-user's capabilities to control the process — normal users can evolve to power users, as opposed to closed environments.

3.3. Concept

²⁵⁵ An effective way to handle complexity is through a model, an abstract representation of a system that enables us to answer questions about it [62]. To create the relevant models, a modeling language will be used, more specifically, the Unified Modeling Language (UML), as it enables the modeling of a variety of artifacts, from software systems to processes and work products [62]. First, ²⁶⁰ the actors of the process are identified as the key agents that interact with it, classified in:

- *Internal* — that takes effective action in the process, namely:
 - *Designer* — idealizes a concept and translates it to a virtual 3D representation (CAD model).
 - *Manufacturer* — takes the virtual 3D model and employs the appropriate materials, techniques and tools to materialize into a physical object.

- *External* — that benefit from or induce actions in the process, e.g.:
 - *Physicist* — studies all physical phenomena in the process and contributes with a greater knowledge about them in the form of physics models and parameters, enabling better control strategies, better materials properties, faster process, etc;
 - *Materials/Mechanical Engineer* — studies all materials/mechanical properties of the produced part in service and contributes usually in the form of empirical knowledge as a set of rules that enhance the part properties and performance;
 - *Control Engineer* — studies the process control, i.e., an effective means of reaching the system goals in a regulated and bounded way, generating the control strategies to be used in the processed [44];
 - *Mathematician* — studies, among other subjects, the manufacturing path topology and the geometric and interchange data representation of the 3D virtual model for the machine execution.
 - *Data Scientist* — studies all process generated data, via data-driven models, leveraging the fact there is an immense quantity of data available to identify data patterns to produce more efficient and accurate empirical knowledge. It can be used to design better experiments, via Design Of Experiments (DOE), and to better control the process, via Artificial Intelligence (AI)[44].

Next, the manufacturing chain was decomposed into four models that will be detailed next, namely: design model, pre-manufacturing model, manufacturing model and post-manufacturing model.

3.3.1. Design Model

Fig. 1 illustrates the design model of the manufacturing chain. The designer initiates this phase by identifying a function/application of the object to be designed. Then, a requirements analysis is performed and the design criteria are

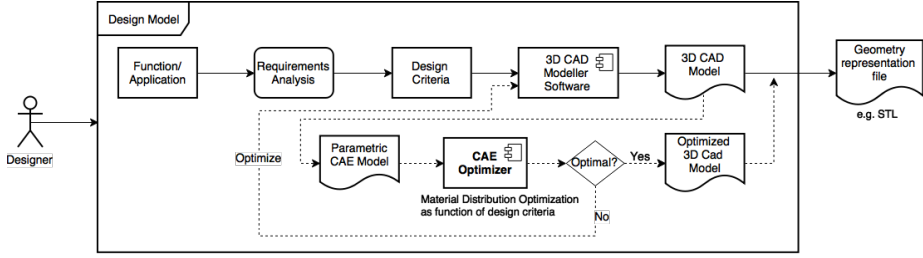


Figure 1: Model of the design activity

established. Now, the object can be modeled in a 3D CAD software, yielding a 3D CAD model of the object. The 3D CAD model ideally, although not necessary, goes through an optimization stage, where it is converted into a parametric CAE model and fed to a CAE optimizer, optimizing the material distribution as a function of the design criteria: if the optimal configuration is not achieved, the designer should optimize the 3D CAD model. Otherwise, for both optimized and unoptimized 3D CAD model, a data file representing the geometry of the 3D CAD is generated, with the most common being an STL file.

3.3.2. Pre-Manufacturing Model

Fig. 2 depicts the pre-manufacturing phase. All internal components of the model are software ones. The manufacturer starts by feeding the geometry representation file to the Computer-Aided Manufacturing (CAM) optimizer (ideal setup — shown in dashed lines) or directly to the slicer (conventional setup — shown in continuous lines). The *CAM optimizer*, as well as the *advisor*, are included as a recommended way of optimizing the manufacturing process: the former is used to optimize it as a function of the process based on systematized knowledge originary from the machine, process and material information; the latter is used to optimize through convenient part orientation, file data sanity check and the conformation to the standards based on empirical knowledge also originary from the machine, process and material information. Both these optional components can be used to optimize the 3D CAD model from the design

stage; however, the first, as it is based on systematized knowledge should issue the recommendations as errors or warnings, stopping the process, while the last, as it based on heuristics and guidelines, should issue them as tips.

Then, the 3D model is sliced using cross xy planes into 2D layers — slicer. Some problems can occur in this stage, especially if the geometry representation file is a tessellation of the surface (STL), as it is unable to accurately represent holes, porosity and discontinuities. This will be addressed in more detail ahead.

The final software component — the post-processor — deserves special attention. The pre-manufacturing and manufacturing models are linked together by a common principle that dates back to the beginning of the Numerical Control (NC) machinery, even before the advent of the computer (and thus the CNC) — the compiler/interpreter. The principle is simple: the instructions to run the machine have to be compiled into a standard code that can be interpreted by the machine (the first was called G-code). Therefore, the code as to be known by both parts — the compiler and the interpreter — represented by language tokens, originating the manufacturing instructions tokens, based on the machine, process and material tokens; the compiler utilize them to compile machine-compliant instruction code; the interpreter is built based on them, incrementing the firmware. The post-processor, before handling the compilation, is also responsible for the layers merging and the inclusion of the process parameters as a means to execute the correct compilation. After the compilation, a file containing machine instructions for manufacturing is generated, which in this case conveniently named *.lcode*.

3.3.3. Manufacturing Model

The manufacturing model, in charge of the manufacturer, includes the control model and the manufacturing process model (Fig. 3) tighly coupled together. The manufacturer feeds the manufacturing instruction file, containing the manufacturing process relevant data for the part fabrication, to the interpreter — a software sub-component of the machine’s firmware. The interpreter then, reads, parses and interprets the *.lcode* instructions. If the End-of-File

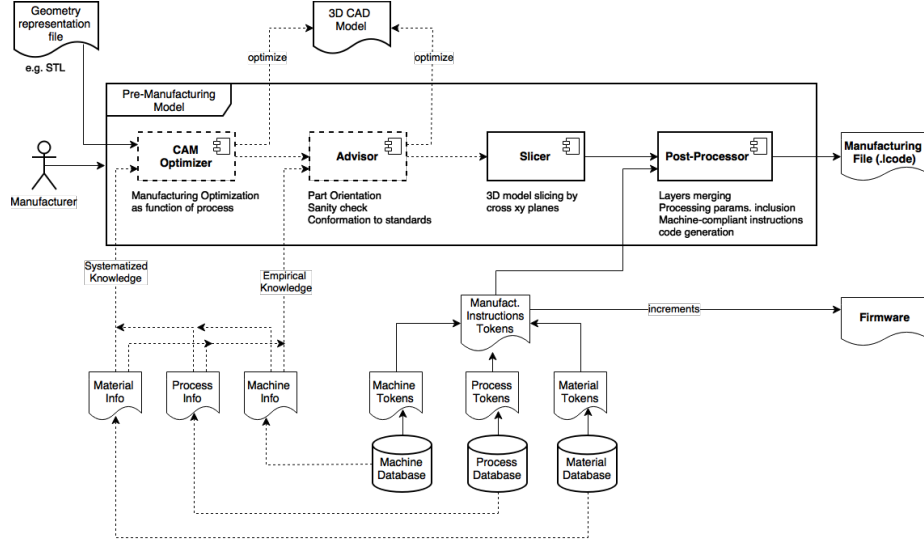


Figure 2: Model of pre-manufacturing activity

(EOF) has not been reached it issues commands to the control board which, in turn, issues controls for the controlled parts like motors, the laser, the heating elements, etc. This yields an effect on the manipulated variable which affects the manufacturing process, represented as a transfer function, different for each process variable. The result of the control action will be a variation in the controlled variable state (e.g., temperature, laser speed, etc.), affecting the manufactured part, which is measured by a sensor (e.g. encoder, thermocouple, pyrometer, etc.) and feed back to the control board for comparison with the desired values for the process variables, with the control action being adjusted accordingly. Additionally, the process variables are registered by another software component — the logger — which reads, converts and logs the relevant parameters as a process info data file to be stored in the process trials database.

When the manufacturing file reaches the end, the part is produced and ready for the next stage — the post-manufacturing phase.

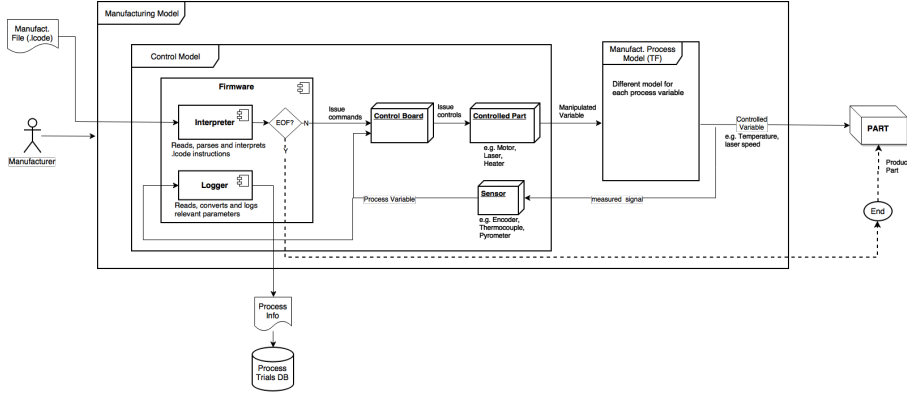


Figure 3: Model of manufacturing activity

3.3.4. Post-Manufacturing Model

The post manufacturing stage (Fig. 4) is probably the most important one in the chain, and often the most neglected, as the quality analysis of the process and of the produced part are conducted in this phase, with the relevant outputs cascading to the precedent stages. With the produced part, the material and mechanical engineers can conduct, respectively, the material analysis and mechanical behaviour analysis; from the former will result the relevant material information and from the latter the mechanical properties of the produced part, to be stored in the respective databases.

The mechanical properties and material information will aid the physicist to conduct the physical analysis via simulation or modeling techniques yielding physical models, which ultimately result in physical laws or theories, predicting what happens or proposing why it happens.

Another often neglected role in the manufacturing chain is of the data scientist which conducts process data analysis, typically in one of two ways: via DOE or AI. Analysing process data history via DOE enables the design of more effective and statistically relevant experiments, resulting in another iteration of the manufacturing phase; analysing via AI enables the recognition of data patterns, yielding empirical models which can lead to empirical laws or theories,

generating heuristics and guidelines that update the *advisor* software component.

The process models will then be generated from both physical and empirical laws/theories that together will the process trials data information enable the control engineer to conduct the control analysis. From this analysis stems an integrated model of the *control + process* combination, which yields control algorithms and parameters. Both these outputs are used to update the machine's firmware and are stored in the process control database. Additionally, they are also used, together with the material information, the mechanical properties and physical laws/theories to update the CAM optimizer.

Lastly, the specification analysis is conducted by the designer and the manufacturer, taken into account the compliance to the function/application in question of the produced part and its mechanical properties. If the function/application is not fulfilled, then the design should be repeated. Otherwise, and if the quality of the part produced namely, mechanical properties, dimensions or surface finishing, etc., is not fulfilled, better manufacturing paths or better process control may be required, leading to a new iteration starting at the pre-manufacturing or manufacturing phases. This information should be properly depured to conveniently and correctly deliver it to the appropriate agent: if the former is verified, this information should be conveyed to the mathematician for topology optimization; if the latter is true, the relevant information should be conveyed to all the agents responsible, directly or indirectly for the control, like the physicist, data scientist and control engineer. If the quality is according to the specifications, the result will be a produced part there is ready for service, and this trial should be signaled as successful, with the relevant information cascading to all databases for further improvement of all involved models.

4. Application of the methodology to 3DMMMLPBF

The proposed methodology is complex and extense, and therefore needs to be implemented by stages, where only the most essential features are considered

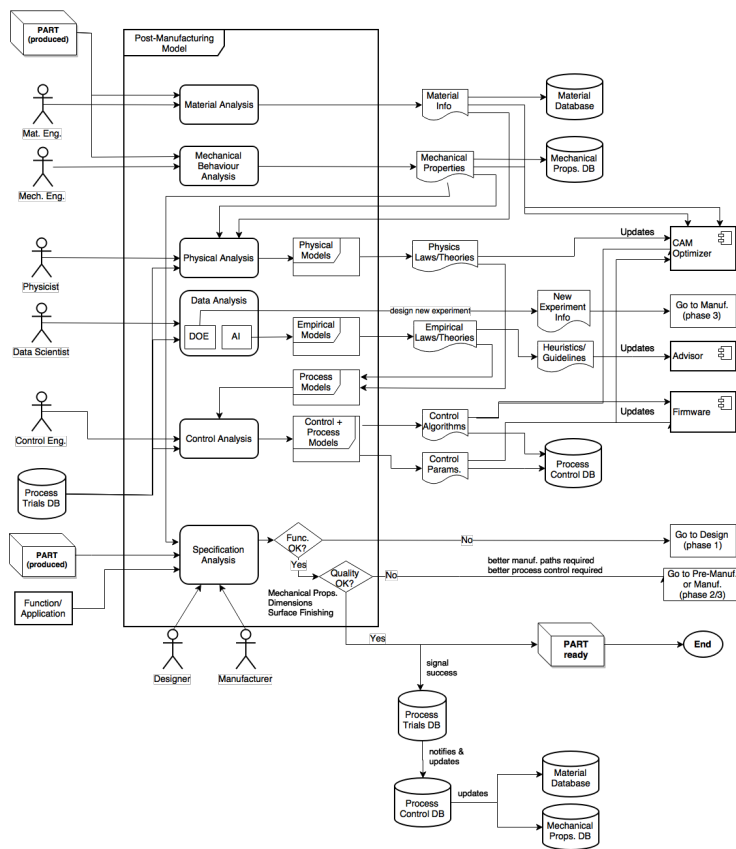


Figure 4: Model of post-manufacturing activity

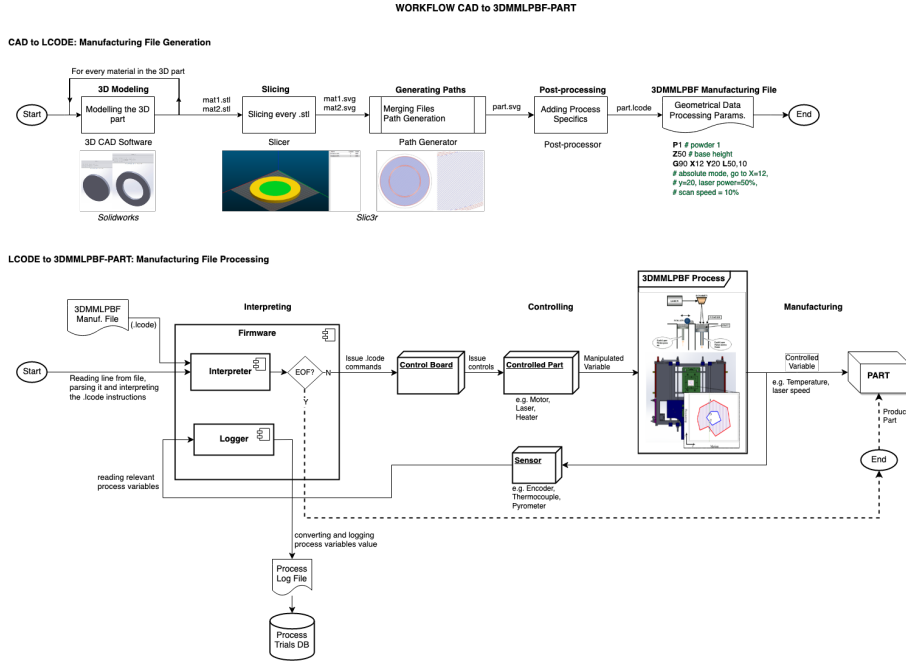


Figure 5: Workflow CAD to 3DMMLPBF-PART

410 in each development phase, being intensively tested before the integration in the framework. Furthermore, the manufacturing process chosen for the multi-material fabrication of tridimensional metallic and composite parts is the LPBF, yielding a novel process named 3DMMLPBF.

415 Thus, a simplified workflow for this process is proposed (fig. 5) as a means to: produce customized 3D multi-material parts with freedom of shape and process control; test the proposed methodology; increase the process's knowledge; quickly iterate over the manufacturing chain with different part's design and different processing solutions, as will be detailed further ahead. This workflow, together with the methodology proposed, paved the way for the correct development and deployment of both software and hardware (mechanical/electronic) components.

420 The workflow — named *CAD to 3DMMLPBF-PART* — integrates the design model and pre-manufacturing model without the CAE and CAM optimiza-

tion steps, respectively, and does not implement the post-processing model yet.
425 This will be reserved for future iterations. The workflow is divided in two phases:
the manufacturing file generation and the manufacturing file processing.

4.1. CAD to LCODE — Manufacturing File Generation

The goal of the first phase — *CAD to LCODE* — of the proposed workflow is
430 the generation of the file containing the manufacturing instructions. Each mate-
rial of the 3D model is modelled individually, in a common 3D CAD modelling
software (e.g. SolidWorks), and a tessellation file of the surface is produced,
containing the geometric information. In this initial stage, the 3D model is
considered to have no holes, porosity or discontinuities, as this would invalidate
435 the usage of the surface tessellation, i.e., the multi-material modelled parts are
considered to be completely filled in.

The next phases — *Slicing and Path Generation* — use an open-source tool
named Slic3r[63], due to the underlying philosophy of transparency, extensibil-
ity, reusability, adaptability, flexibility, and modularity desired. Furthermore,
Slic3r is a highly configurable and robust slicer, allowing for the fine control of
440 the multiple types of scan paths — rectilinear, line, concentric, 3D honeycomb,
Hilbert Curve, etc.—, generating customized G-code for multiple target plat-
forms and scriptable (for batch mode). We will be working with a cloned version
of the project to integrate the custom scan paths algorithms. Additionally, pre-
scanning paths will be added to deal with the high thermal gradients induced in
445 a single passage of the laser beam. The output of both these phases is an Scal-
able Vector Graphics (SVG) file; the choice of this file format is due to the use of
markup language, namely eXtensible Markup Language (XML), for describing
two-dimensional vector and mixed vector/raster graphics[64]. This allows the
conveying of extra information besides the geometry, that can be packed in a
450 structure node, for example line color attribute to represent different materials,
addressing the multi-material representation ambiguity. In respect of the oper-
ations’ logic, each material is sliced in layers and output as a SVG file. Then
the files are combined for each layer and the scan paths are generated, yielding

a complete SVG file of the part.

455 This file, containing the geometry information pertaining to the scan paths,
will be post-processed to add the process relevant parameters, like material and
process parameters with the former being pulled from the material database
and the latter being defined by the end-user. The result will be a file — `.lcode`
— containing the manufacturing instructions for the 3DMMLPBF process with
460 the geometrical data and process parameters. The post-processor is currently
under development, but an extract sample is provided in 5, illustrating the
tokens used:

- P1 — Powder 1
 - Z50 — base height
- 465 • G90 X12 Y20 L50,10 — absolute mode, go to X=12, Y=20, with laser
power at 50% and scan speed at 10%.

4.2. *LCODE to 3DMMLPBF-PART — Manufacturing File Processing*

The goal of the second phase — *LCODE to 3DMMLPBF-PART* — of the
proposed workflow is the processing of the file containing the manufacturing
470 instructions. This file will be read line-by-line, parsed and interpreted, issuing
commands to the control board based on the *lcode* instructions of the file. The
remainder of the operation — controlling and manufacturing — is similar to the
one described in the manufacturing model (Section 3.3.4), with the controlled
part inducing an effect in the 3DMMLPBF process and the controlled variable
475 that affects the manufactured part being measured and logged by the logger
software component to a process log file, which is stored in the process trials
database. When the *End-of-File* is reached, the process terminates and the part
is manufactured.

This workflow represents the typical simplified one for the 3DMMLPBF
480 manufacturing process. However, currently there is a major restriction for the
implementation of this workflow as is, due to the closed nature of the proprietary
software of our CO₂, YAG-Nd and fiber lasers. In the future, we will implement

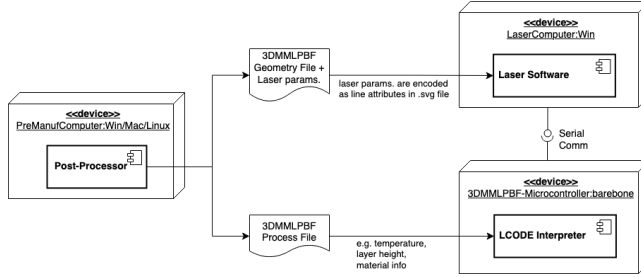


Figure 6: Workaround for the proposed workflow: two separate data files — geometry and process — are used by the laser software and LCODE interpreter for scanning paths marking and process related tasks, respectively

our own software to control the lasers hence integrating in the 3DMMMLPBF machine, but for now a workaround was used. This workaround consists in separating the geometric data from the process data at the post-processing stage and assigning it, respectively, to the laser and the 3DMMMLPBF machine. The processing parameters of the laser are encoded in the SVG file as line attributes that the laser software is able to recognize and use for the scan paths marking.

Fig. 6 illustrates the architecture of this solution with the representation of the data streams, the software components that use those streams, the hardware nodes where the software components are assigned and the protocols under which they communicate, namely serial communication for laser and 3DMMMLPBF machine synchronization.

4.3. 3DMMMLPBF machine for multi-material processing

Based on the requirements imposed by the 3DMMMLPBF process, namely the freedom of shape and of control and the specifics of the multi-material processing, an equipment was developed and built (version 2.0), as illustrated in Fig. 7. This equipment is a more compact version, optimizing powder consumption and recovery, and manufacturing efficiency.

The equipment includes: the *powder recoating system*; the *powder reservoirs*; the *heating elements* for bed and reservoirs heating; *powder recovery system*

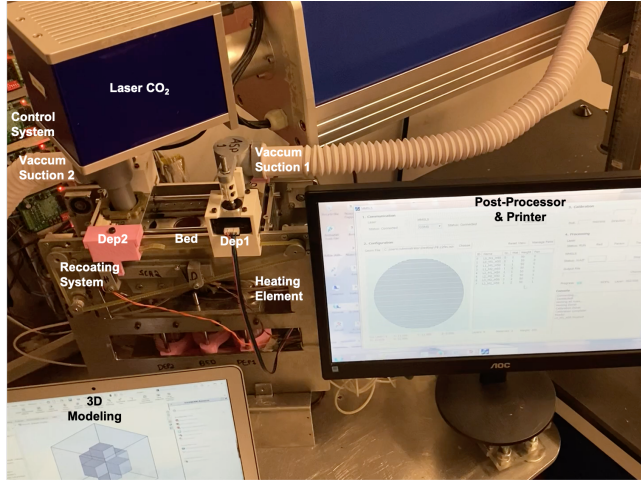


Figure 7: 3DMMLPBF machine — version 2.0

consisting of a vacuum suction system; *atmosphere control system* consisting of a pressurized inert gas system; and the *control system*.

The working principle is similar to one of the typical LPBF machines, but
505 it includes some tweaks for multi-material processing:

1. the printing bed lowers by layer height;
2. the powder reservoir goes up by layer height and powder is dragged by the recoating system to the printing bed; machine signals to the laser that it is ready for printing;
3. the laser marks the scanning paths; when a layer is finished or material changes the geometry file changes layer and the laser stops; the laser signals this fact to the machine;
- 510 4. the machine proceeds with the *lcode* instructions processing: if a new material is needed, the powder is recovered via powder recovery system and a new material is fetched from the respective reservoir and fed to the printing bed; the machine signals to the laser that is ready for printing;
- 515 5. the process repeats itself for each new layer and for each new material in a layer until the *End-of-File* is reached.

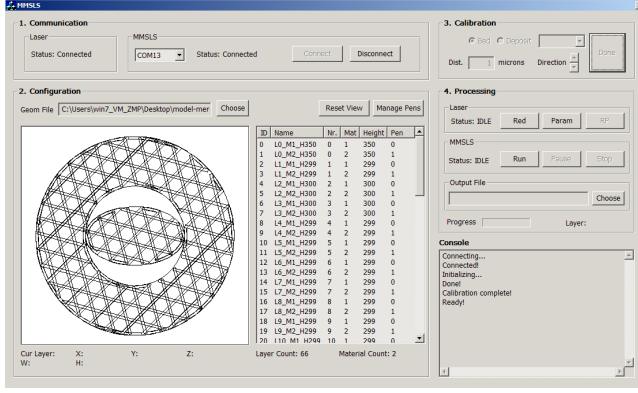


Figure 8: GUI to interface the 3DMMMLPBF machine

It should be noted that, due to selective each material before a new one is
520 added, the processing paradigm shifts from layer to layer to a point-by-point manufacturing.

A Graphical User Interface (GUI) was developed (Fig. 8) to interface the 3DMMMLPBF machine, comprising the following software artifacts: post-processor — maps the geometrical data into process parameters through associated pens; printer — handles the communication with the equipment, command interpretation and data logging.
525

Table 1 lists the 3DMMMLPBF machine specifications.

Lastly, the post-manufacturer software was developed to feedback relevant information to all agents in the manufacturing chain. Fig. 9 illustrates the 530 manufacturing model view, comprising the model, the scan pattern, its layers and the associated materials and pens. The manufacturing model can be loaded and previewed, alongside with the manufacturing output file (the output from the equipment). The top-level entities are shown as the top tabs, namely part, 3D model, manufacturing model, laser, and mechanical tests. All databases can 535 be exported separately for appropriate handling by each process' agent.

Table 1: 3DMMLPBF machine final specifications

Dimensions (l x w x h)[mm]	320 x 100 x 400
Power supply	Laser: 400 VAC, 10 A Machine: 24 V, 15 A
Build dimensions [mm]	25Ø x 100
Nr. of materials	2
Temperature	Tested up to 250°C (higher temperatures can be used)
Laser	Type: CO_2 Power: 30 W Spot size: 50 μm
Resolution [μm]	Full-step (all axes, except bed): 5 ± 0.25 1/16-step (bed): 0.32 ± 0.016
Estimated cost [EURO]	Laser: 7500 Machine: 1500 Total: 9000

5. Tests

In this chapter, the 3DMMLPBF methodology devised was tested and the results are presented, namely: tests to the software toolchain instantiated and the workflow, and equipment and product manufacturing tests.

5.1. Workflow

The workflow tests contemplate two types of tests: unit tests — tests to each software component independently, to assess if the functionality of each component meets its specific requirements; integrated tests — tests to the pipelining of the software components, to assess if the overall workflow specifications are met.

545

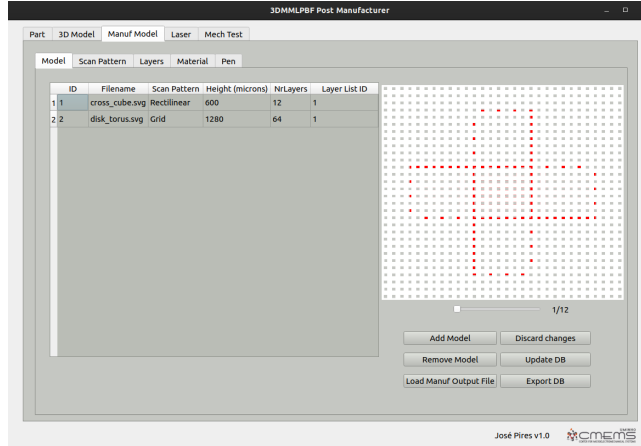


Figure 9: 3DMLLPBF Post-Manufacturer

5.1.1. Slicer and Path generator

The unit tests performed fall in the following categories: different path topologies; different slicing and path generation parameters; different 3D models.

550 The `.stl` input models used for the testing were: `mod1.stl` — a torus, simply called a *ring*; `mod2.stl` — a disk (see fig. 10). These models aims to represent two different materials and the simplest of the cases of multi-material processing: filled and unfilled regions without overlapping, but close enough that the bonding can occur via welding.

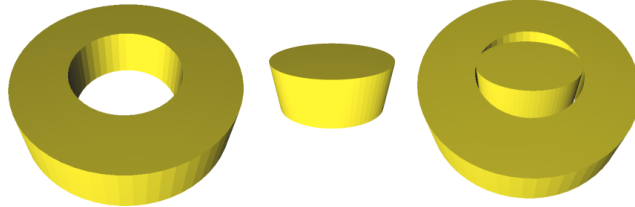


Figure 10: Input `.stl` models: `mod1.stl` (left); `mod2.stl` (center); assembled (right)

555 *Path topologies.* The slicer supports different path topologies, namely: rectilinear; aligned-rectilinear; grid; triangles; cubic; concentric; honeycomb 3d-

honeycomb; hilbert-curve; archimedean-chords; octagram-spiral.

Due to intrinsic open nature of the slicer and path generator, shell scripting was used to automatically test all path topologies in a batch.

As a common denominator between the tests, the following main parameters were fixed (see table 2): fill angle, fill density and infill extrusion width. The path topologies tests results are presented in fig. 11 for the different topologies. It can be seen that the slicer + path generator is able to generate the different topologies for multi material components.

Table 2: Path topology main fixed parameters

fill angle	fill density	infill extrusion width
45°	15 %	0.1 mm

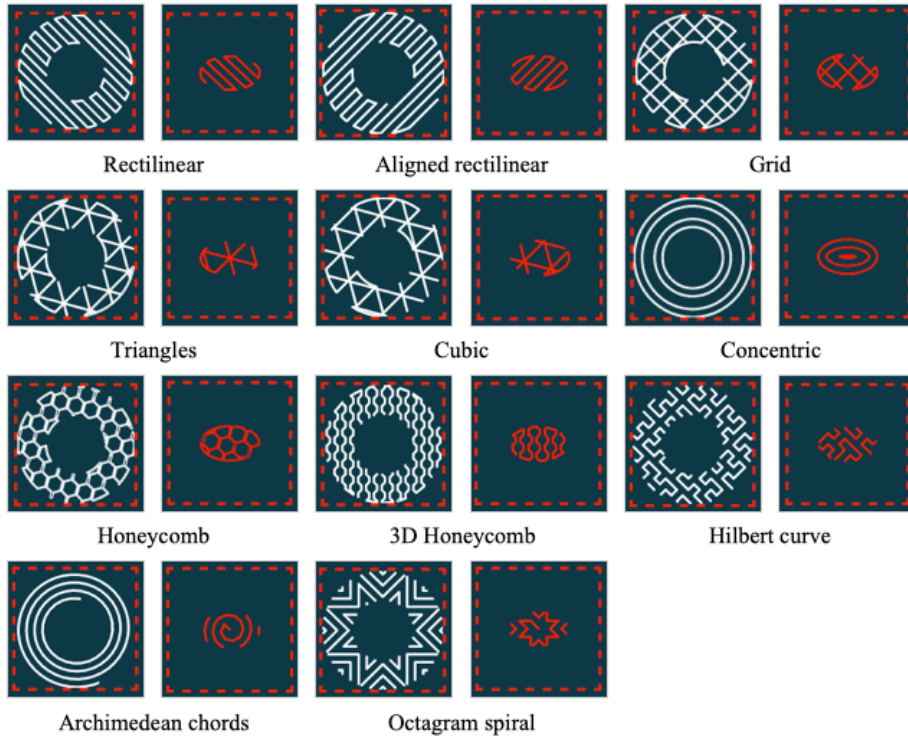


Figure 11: Path topologies test

565 *Slicing and Path generation parameters.* For the slicing and path generation parameters testing the 3D models are the same and the path topology selected was the rectilinear one. The following parameters were varied: fill angle, fill density, infill extrusion width (for path generation); layer height (for slicer). Once again, the scripting technique previously mentioned was used.

570 The fill angle was varied from 0% to 90%. Only one material is presented, as the slicing and path generation for multi material was previously validated. As can be seen in fig. 12, the fill angle is successfully modified.

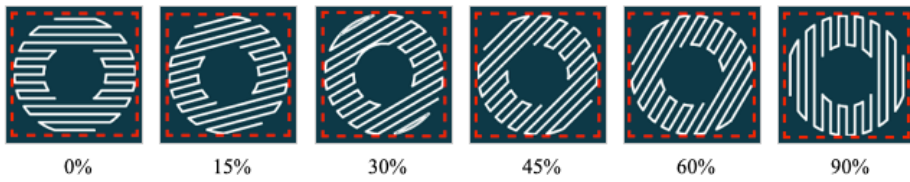


Figure 12: Fill angle test: 0% to 90%

575 The fill density was varied from 1% to 40%. As can be seen in fig. 13, for very low fill densities, e.g. 1–5%, the slice is only partially filled; increasing the fill density from 20 to 40%, the slice is almost completely filled. These higher fill densities (40% for the models in analysis) can be helpful in enabling the porting of the 3D printing path topologies to SLS ones, as the reduced distance between fillings (fill spacing) helps to promote powder melting in small gaps.

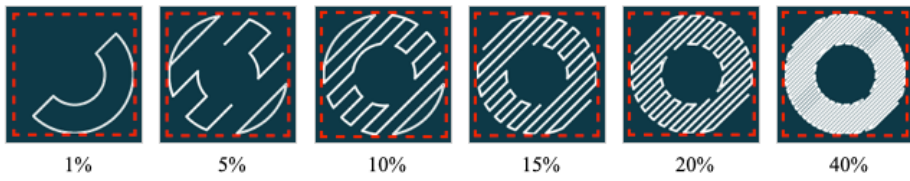


Figure 13: Fill density test: 1% to 40%

580 The infill extrusion width was varied from 0.01 to 0.5 millimeters. As can be seen in fig. 14, for very low extrusion widths, e.g. 0.01–0.02 mm, the slice is almost completely filled, which can be beneficial for SLS paths. For higher infill extrusions widths, e.g. 0.5 mm, the part is only partially filled.

Although related, fill density and infill extrusion width are conceptually different: infill extrusion width is the filling width, which can be lowered to mimic the laser marking path width; fill density is the amount of filling paths per slice area.

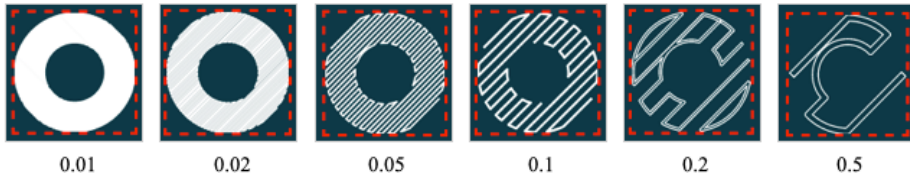


Figure 14: Infill extrusion width test: 0.01–0.5 mm

To analyse the slicer performance, the layer height was varied from 0.025 to 0.001 millimeters, and the number of layers, execution time, and file size were registered in table 3. As can be seen, for 25 micrometers, the number of layers is 120, taking 2.86 seconds to compute and yielding a file size of 1.3 MB. Decreasing the layer height, increases the number of layers as expected, as well as the computation time and file size. Even more interesting is that the slicer is capable of slicing layers with 1 micrometer height within a reasonable amount of time (79.4 seconds), which excels the fabrication requirements. However, the file size is penalised as expected, yet, is still tolerable.

Table 3: Layer height tests: 0.025–0.001 mm

Layer height [mm]	Nr. of layers	Computation time [s]	File Size [kB]
0.025	120	2.86	1300
0.020	150	3.84	1600
0.015	198	5.52	2100
0.010	298	7.12	3100
0.005	592	14.50	6200
0.001	1456	79.39	29400

Models. In this section is analysed the response of the slicer and path generation to different input models:

- *Cross and cube*: a bi-material component with an internal cavity belonging to one material and the external component to another; this is a good example of a multi-material component that is only feasible via additive manufacturing (fig. 15);
 - *3 cubes*: a three material component, with each cube being enclosed by an outer one. Once again, this a typical example of a component only feasible using AM (fig. 17).
- Furthermore, the integrity of the `.stl` file format produced and the agnostic behaviour of the slicer and path generator in respect of the inputs was tested by using a different 3D CAD modelling tool — FreeCAD — an open source 3D parametric modeller [65].

The cross and cube component 3D model is illustrated in fig. 15. Consists of a cross of one material inserted in a cube of another material. The component was exported as two `.stl` files corresponding to each material and fed to the the slicer and path generator, using the default values. The result can be seen in fig.16, with both sub-components being sliced and filled with the rectilinear pattern in consecutive layers corresponding to the center of the part. Thus, the slicer and path generator performs well with a different input model and is agnostic about the provenance of the `.stl` input files.

The 3 cubes 3D model is illustrated in fig. 17. Consists of a three cubes, each one inside of the outer one. The component was exported as three `.stl` files corresponding to each material and fed to the the slicer and path generator, using the default values. The result can be seen in fig.18, with all sub-components being sliced and filled with the rectilinear pattern in consecutive layers corresponding to the three materials. An excerpt of the output `.svg` file is presented in Listing 1, where it can be seen that the slicing and path generation occurred for all three materials.

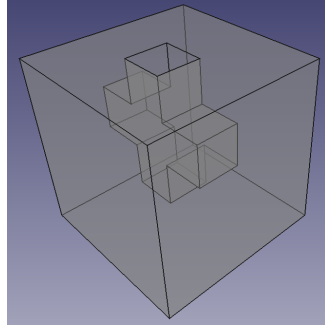


Figure 15: Cross and Cube 3D model

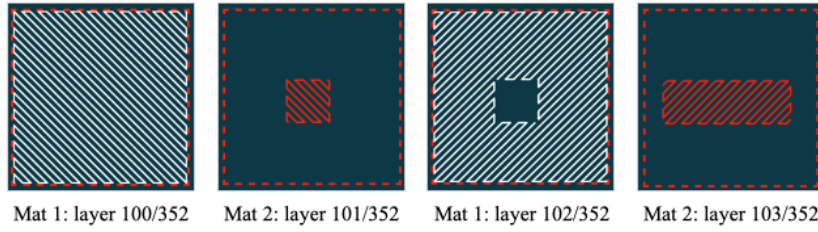


Figure 16: Cross and cube slicing test

625 Once again, the slicer and path generator performs well with a different input
 model and is agnostic about the provenance of the `.stl` input files. Furthermore,
 it is capable of handling models with more than two materials.

```

630 <g id="L0_M1_H25" slic3r:z="0.0250" slic3r:slice-z="0.0125" slic3r:layer-height=
      "0.0250" slic3r:mat="1">
<polyline points= "20,0 0,0 0,20 20,20 20,0 " style="fill: none; stroke: white;
      stroke-width: 0.1; fill-type: evenodd" slic3r:type="" />
</g>
635 <g id="L0_M2_H25" slic3r:z="0.0250" slic3r:slice-z="0.0125" slic3r:layer-height=
      "0.0250" slic3r:mat="2">
<polyline points= "15,5 0,5 0,20 15,20 15,5 " style="fill: none; stroke: red;
      stroke-width: 0.1; fill-type: evenodd" slic3r:type="" />
</g>
640 <g id="L0_M3_H25" slic3r:z="0.0250" slic3r:slice-z="0.0125" slic3r:layer-height=
      "0.0250" slic3r:mat="3">
<polyline points= "10,10 0,10 0,20 10,20 10,10 " style="fill: none; stroke: blue
      ; stroke-width: 0.1; fill-type: evenodd" slic3r:type="" />
</g>
```

Listing 1: 3cubes.svg (excerpt)

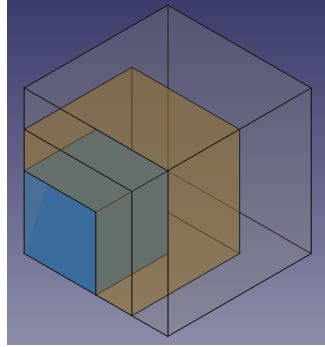


Figure 17: 3 cubes 3D model

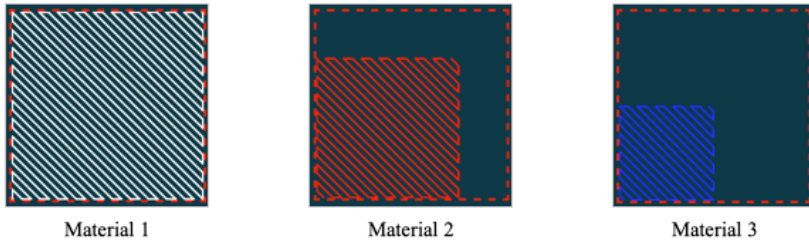


Figure 18: 3 cubes slicing test

645 5.1.2. Discussion

The workflow tests performed on the slicer and path generator, and on the post-processor and printer, helped to improve the respective tools by feeding back relevant information. More importantly, these tests allowed to validate the toolchain:

- 650 • Slicer and path generator: the slicer and path generator are capable of slicing and generating paths for various 3D models with different fill angle, fill density, infill extrusion width, layer height, and number of materials. The slicer is agnostic about the input files. It was also seen that a significant number of path topologies are available and that the fill density and infill extrusion width can be varied to mimic the required path filling for laser trajectories. Due to the high number of path topologies available off-the-shelf and the possible adaptation from the 3D printing area to

the SLS one, fast iteration on part production is possible. Lastly, due to
660 the open source nature of the slicer and path generator, the modification
of the available path topologies or the addition of new ones is relatively
straightforward.

- 665
- Post-processor and printer: the post-processor is capable of processing the geometric and material data in the manufacturing file and mapping them to the desired processing parameters, irrespective of the material, layer height and layer number. The printer was successfully tested on offline mode to produce the part. Additionally, it was also seen the tight coupling between post-processor and printer, signalled by the restriction on the production of parts with more than two materials.

5.2. Equipment and Manufacturing

670 In this section the tests conducted on the equipment and part manufacturing are presented. As a proof-of-concept, the cross and cube model was used. This bimaterial model was sliced in 6 layers for easier process demonstration, with a height of 50 micrometers and the rectilinear toolpath was used. For easier demonstration, the same material was used, but with different colors for better
675 visualization.

The resulting manufacturing model was then loaded to the Post-Processor and Printer GUI as illustrated in Fig. 19. The master system is connected to the 3DMMLPBF machine via COM port. The process parameters are mapped to each material through the **Manage Pens** pushbutton, as depicted in Table 4.
680 A calibration can also be performed to minimize powder usage. After all these steps are completed and the machine homing is done, the manufacturing can start by pressing the **Run** pushbutton.

Fig 20 illustrates the manufacturing: on the left the visualization of the current layer and the corresponding GUI status; on the right the result of the
685 layer after being printed. As it can be seen, the layer is correctly printed, in compliance with the process and geometrical data provided.

Table 4: Manufacturing parameters for each material

Process Parameters	Mat 1 (Purple)	Mat 2 (Black)
Speed [mm/s]	850	1000
Power (%)	45	25
Pulse frequency (kHz)	20	20

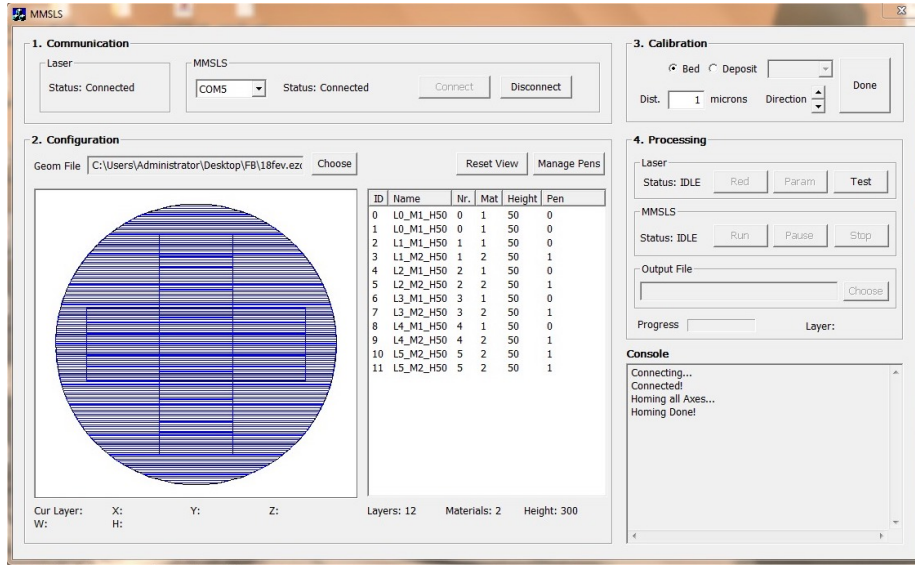


Figure 19: Post-Processor & Printer GUI: Initialization

Finally, Fig. 21 illustrates the bimaterial cross and cube part produced after being cross-sectioned, where it is clearly visible the tridimensional material variation, as defined by the original 3D CAD model. Furthermore, the Scanning Electron microscope (SEM) analysis performed on the part (Fig. 22) showed good densification, demonstrating the good manufacturing performance of the equipment.

Additionally, the 3DMMLPBF equipment was tested in conjunction with a fiber laser to verify its agnosticism. Unfortunately, no suitable powder material was available, thus the tests comprised only the scanning paths and process parameters. This test was successful, proving the 3DMMLPBF can be used with multiple lasers without any modification. Hence, this opens new prospects on

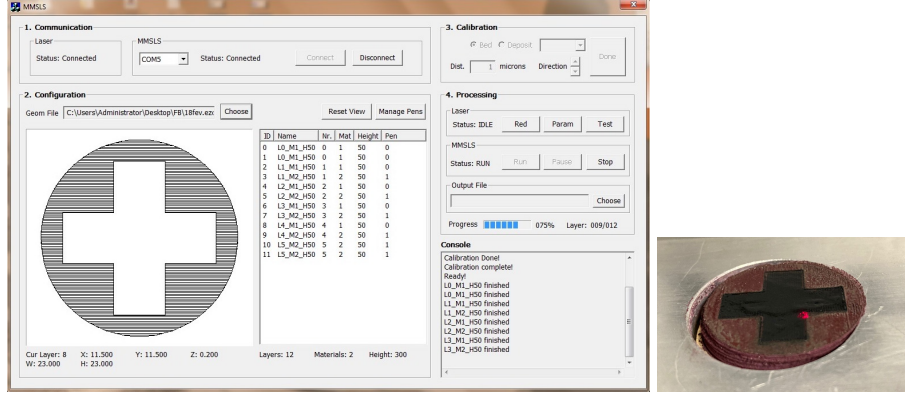


Figure 20: Post-Processor & Printer: Manufacturing

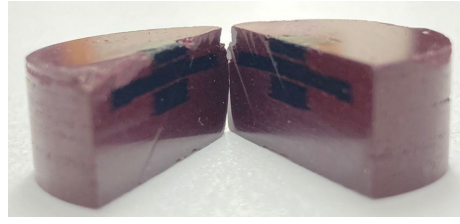


Figure 21: Cross and cube part: final result

the use of the equipment, where the combination of multiple laser sources of different wavelength can further support the fabrication of multi-material components of very distinct powder granulometric size, contingent of their flowability and an adequate powder dispensing system.

The equipment and manufacturing tests performed clearly demonstrate the feasibility of 3DMMLPBF process and validate the equipment developed, as well as the accompanying toolchain.

6. Conclusion

Current LPBF based processes' workflow lies in a closed environment that does not take into account all involved agents, limiting their access to relevant information which consequently hinders the technological development. Fur-

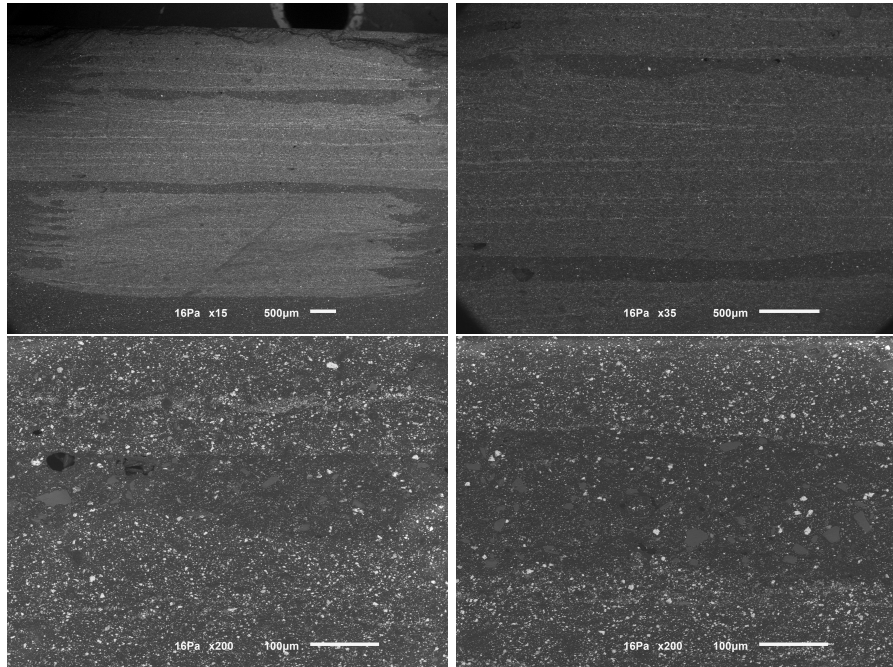


Figure 22: Cross and cube part: SEM analysis

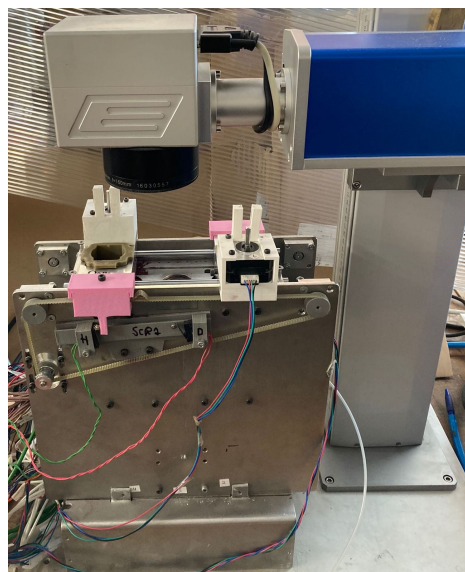


Figure 23: Laser agnostic: the 3DMMLPBF equipment was tested with a fiber laser

thermore, as often this workflow resides in the chaining of intransparent blocks
710 of software and/or hardware, the complexity is very difficult to handle, as it does not provide a flexible, modular and reusable infrastructure. If one adds the multi-material processing to this already complex equation, it becomes nearly impossible to handle.

The transparency of the tools used and a deep level of control over them,
715 alongside with a systematic and global perspective of LBAM processes without the limitation of specific tools is of the utmost importance. Thus, in the present work a methodology is proposed in order to cope with the identified difficulties and to provide some desirable features, namely: abstraction, modularity, flexibility, extensibility, high customisation, capability of managing the different
720 information flows, guidance to end-users and maximization of process's control. This methodology works by considering the relevant actors in LPBF processes and the relevant data flows and their transformation in the manufacturing chain. Four models were created for this purpose: design, pre-manufacturing, manufacturing and post-manufacturing. As a result, the information flows are
725 conveniently and accurately handled by the relevant agent improving the manufacturing chain, and the software components and hardware components were identified.

Then, this methodology was applied specifically to the LPBF process for multi-material processing. A simple workflow was presented with the minimum
730 features required for the task, implementing the pre-manufacturing, manufacturing stages and post-manufacturing stages, whereas the optimizations will be implemented in the near future. Based on this methodology an equipment for LPBF multi-material processing was designed and built.

Lastly, tests were conducted over the workflow, and equipment and manufacturing, proving the feasibility and correctness of the methodology and the associated outputs — the software toolchain and the equipment — for the production of 3D multi-material components by the LPBF process.
735

7. Future work

In the near future the remainder of the methodology will be implemented.
740 The optimizations in the manufacturing chain will be addressed by the inclusion of the CAE and CAM optimizers, as well as the advisor.

Concerning the 3DMMLPBF equipment developed, the intention is to replace the laser software by our own custom software, enabling the integration of the laser in the current equipment yielding a unique equipment for multi-material processing. This will enable the generation of a single *lcode* file with
745 manufacturing instructions and reduce the complexity of the software components and the synchronization protocol involved, while providing a deeper level of control and customisation. As a result, the post-processor will be optimized.

It is also expected that the post-manufacturing chain will allow improvements in the manufacturing chains by performing the relevant analysis. Lastly,
750 some additional solutions for multi-material processing and specially MMFGMs will be tested based on different hardware and software solutions — e.g., combination of multiple laser sources — which is supported by the modularity and flexibility features of the proposed methodology, at both the software and hardware level.
755

Declaration of Competing Interest

The authors declare that they have no known competing financial interests or personal relationships that could have appeared to influence the work reported in this paper.

760 Acknowledgements

This work was supported by Portuguese Foundation of Science and Technology national funds, under the national support to R&D units grant, through the reference projects UIDB/04436/2020 and UIDP/04436/2020), and also, through the project ‘HAMaBICo — Hybrid Additive Manufacturing for Bio-Inspired

⁷⁶⁵ Components', reference NORTE-01-0145-FEDER-000018 and by the project Add.Additive_Manufacturing to Portuguese Industry_POCI-01-0247-FEDER-024533.

References

- [1] G. Liu, X. Zhang, X. Chen, Y. He, L. Cheng, M. Huo, J. Yin, F. Hao, S. Chen, P. Wang, et al., Additive manufacturing of structural materials, Materials Science and Engineering: R: Reports 145 (2021) 100596.
- [2] O. Carvalho, M. Buciumeanu, S. Madeira, D. Soares, F. Silva, G. Miranda, Optimization of alsi–cnts functionally graded material composites for engine piston rings, Materials & Design 80 (2015) 163–173.
- ⁷⁷⁰ [3] T. Wohlers, Wohlers report 2011: Additive manufacturing and 3d printing, state of the industry, wohlers associates, ft, Collins, CO.
- [4] H. Chen, Y. Sun, W. Yuan, S. Pang, W. Yan, Y. Shi, A review on discrete element method simulation in laser powder bed fusion additive manufacturing, Chinese Journal of Mechanical Engineering: Additive Manufacturing Frontiers (2022) 100017.
- ⁷⁸⁰ [5] M. Bayat, W. Dong, J. Thorborg, A. C. To, J. H. Hattel, A review of multi-scale and multi-physics simulations of metal additive manufacturing processes with focus on modeling strategies, Additive Manufacturing 47 (2021) 102278.
- [6] B. Xiao, Y. Zhang, Numerical simulation of direct metal laser sintering of single-component powder on top of sintered layers, Journal of Manufacturing Science and Engineering 130 (4) (2008) 041002.
- [7] K. Dai, L. Shaw, Thermal and mechanical finite element modeling of laser forming from metal and ceramic powders, Acta Materialia 52 (1) (2004) 69–80.

- [8] X. He, J. Mazumder, Transport phenomena during direct metal deposition, Journal of Applied Physics 101 (5) (2007) 053113.
- [9] X. He, G. Yu, J. Mazumder, Temperature and composition profile during double-track laser cladding of h13 tool steel, Journal of Physics D: Applied Physics 43 (1) (2009) 015502.
- [10] A. Manthiram, D. Bourell, H. Marcus, Nanophase materials in solid freeform fabrication, JOM Journal of the Minerals, Metals and Materials Society 45 (11) (1993) 66–70.
- [11] H. Asgharzadeh, A. Simchi, Effect of sintering atmosphere and carbon content on the densification and microstructure of laser-sintered m2 high-speed steel powder, Materials Science and Engineering: A 403 (1) (2005) 290–298.
- [12] P. Avrampos, G.-C. Vosniakos, A review of powder deposition in additive manufacturing by powder bed fusion, Journal of Manufacturing Processes 74 (2022) 332–352.
- [13] D. Gu, W. Meiners, K. Wissenbach, R. Poprawe, Laser additive manufacturing of metallic components: materials, processes and mechanisms, International materials reviews 57 (3) (2012) 133–164.
- [14] S. M. Thompson, L. Bian, N. Shamsaei, A. Yadollahi, An overview of direct laser deposition for additive manufacturing; part i: Transport phenomena, modeling and diagnostics, Additive Manufacturing 8 (2015) 36–62.
- [15] Y. Tadjdeh, Navy beefs up 3d printing efforts with new ‘print the fleet’ program, National Defense 99 (731) (2014) 24–26.
- [16] M. J. Foust, D. Thomsen, R. Stickles, C. Cooper, W. Dodds, Development of the ge aviation low emissions taps combustor for next generation aircraft engines, AIAA Paper 936 (2012) 2012.
- [17] R. Scott, Chinese Company Showcases Ten 3D-Printed Houses, ArchDaily, <http://www.archdaily.com/543518/>

chinese-company-showcases-ten-3d-printed-houses, accessed:
2017-09-25 (2014).

- 820 [18] K. Dalgarno, T. Stewart, Production tooling for polymer moulding using
the rapidsteel process, *Rapid Prototyping Journal* 7 (3) (2001) 173–179.
- [19] L.-E. Rännar, A. Glad, C.-G. Gustafson, Efficient cooling with tool inserts
manufactured by electron beam melting, *Rapid Prototyping Journal* 13 (3)
(2007) 128–135.
- 825 [20] L. Murr, S. Gaytan, F. Medina, H. Lopez, E. Martinez, B. Machado,
D. Hernandez, L. Martinez, M. Lopez, R. Wicker, et al., Next-generation
biomedical implants using additive manufacturing of complex, cellular and
functional mesh arrays, *Philosophical Transactions of the Royal Society of
London A: Mathematical, Physical and Engineering Sciences* 368 (1917)
(2010) 1999–2032.
- 830 [21] R. McCann, M. A. Obeidi, C. Hughes, É. McCarthy, D. S. Egan, R. K.
Vijayaraghavan, A. M. Joshi, V. A. Garzon, D. P. Dowling, P. J. McNally,
et al., In-situ sensing, process monitoring and machine control in laser
powder bed fusion: A review, *Additive Manufacturing* 45 (2021) 102058.
- 835 [22] B. Vayre, F. Vignat, F. Villeneuve, Metallic additive manufacturing: state-
of-the-art review and prospects, *Mechanics & Industry* 13 (2) (2012) 89–96.
- [23] D. Salehi, M. Brandt, Melt pool temperature control using labview in nd:
Yag laser blown powder cladding process, *The international journal of advanced
manufacturing technology* 29 (3) (2006) 273–278.
- 840 [24] T. Purtonen, A. Kalliosaari, A. Salminen, Monitoring and adaptive control
of laser processes, *Physics Procedia* 56 (2014) 1218–1231.
- [25] M. Vaezi, S. Chianrabutra, B. Mellor, S. Yang, Multiple material additive
manufacturing—part 1: a review: this review paper covers a decade of
research on multiple material additive manufacturing technologies which

- 845 can produce complex geometry parts with different materials, *Virtual and Physical Prototyping* 8 (1) (2013) 19–50.
- [26] D. Han, H. Lee, Recent advances in multi-material additive manufacturing: Methods and applications, *Current Opinion in Chemical Engineering* 28 (2020) 158–166.
- 850 [27] A. Bandyopadhyay, B. Heer, Additive manufacturing of multi-material structures, *Materials Science and Engineering: R: Reports* 129 (2018) 1–16.
- [28] D. Joung, V. Truong, C. C. Neitzke, S.-Z. Guo, P. J. Walsh, J. R. Monat, F. Meng, S. H. Park, J. R. Dutton, A. M. Parr, et al., 3d printed stem-cell derived neural progenitors generate spinal cord scaffolds, *Advanced functional materials* 28 (39) (2018) 1801850.
- 855 [29] Y. Lu, S. N. Mantha, D. C. Crowder, S. Chinchilla, K. N. Shah, Y. H. Yun, R. B. Wicker, J.-W. Choi, Microstereolithography and characterization of poly (propylene fumarate)-based drug-loaded microneedle arrays, *Biofabrication* 7 (4) (2015) 045001.
- 860 [30] F. Li, N. P. Macdonald, R. M. Guijt, M. C. Breadmore, Multimaterial 3d printed fluidic device for measuring pharmaceuticals in biological fluids, *Analytical chemistry* 91 (3) (2018) 1758–1763.
- [31] F. Bartolomeu, M. Costa, N. Alves, G. Miranda, F. S. Silva, Additive manufacturing of niti-ti6al4v multi-material cellular structures targeting orthopedic implants, *Optics and Lasers in Engineering* 134 (2020) 106208.
- 865 [32] G. Coelho, T. M. F. Chaves, A. F. Goes, E. C. Del Massa, O. Moraes, M. Yoshida, Multimaterial 3d printing preoperative planning for frontoethmoidal meningoencephalocele surgery, *Child's Nervous System* 34 (4) (2018) 749–756.
- 870 [33] A. Cresswell-Boyes, A. Barber, D. Mills, A. Tatla, G. Davis, Approaches to 3d printing teeth from x-ray microtomography, *Journal of Microscopy* 272 (3) (2018) 207–212.

- [34] A. Sydney Gladman, E. A. Matsumoto, R. G. Nuzzo, L. Mahadevan, J. A. Lewis, Biomimetic 4d printing, *Nature materials* 15 (4) (2016) 413–418.
- 875 [35] C. Yuan, D. J. Roach, C. K. Dunn, Q. Mu, X. Kuang, C. M. Yakacki, T. Wang, K. Yu, H. J. Qi, 3d printed reversible shape changing soft actuators assisted by liquid crystal elastomers, *Soft Matter* 13 (33) (2017) 5558–5568.
- 880 [36] D. Espalin, D. W. Muse, E. MacDonald, R. B. Wicker, 3d printing multifunctionality: structures with electronics, *The International Journal of Advanced Manufacturing Technology* 72 (5) (2014) 963–978.
- [37] A. D. Valentine, T. A. Busbee, J. W. Boley, J. R. Raney, A. Chortos, A. Kotikian, J. D. Berrigan, M. F. Durstock, J. A. Lewis, Hybrid 3d printing of soft electronics, *advanced Materials* 29 (40) (2017) 1703817.
- 885 [38] W. HuangáGoh, A. HoseináSakhaei, et al., Highly stretchable hydrogels for uv curing based high-resolution multimaterial 3d printing, *Journal of Materials Chemistry B* 6 (20) (2018) 3246–3253.
- 890 [39] T.-S. Wei, B. Y. Ahn, J. Grotto, J. A. Lewis, 3d printing of customized li-ion batteries with thick electrodes, *Advanced Materials* 30 (16) (2018) 1703027.
- [40] F. Brueckner, M. Riede, M. Müller, F. Marquardt, R. Willner, A. Seidel, E. Lopéz, C. Leyens, E. Beyer, Enhanced manufacturing possibilities using multi-materials in laser metal deposition, *Journal of Laser Applications* 30 (3) (2018) 032308.
- 895 [41] K. Shah, I. ul Haq, A. Khan, S. A. Shah, M. Khan, A. J. Pinkerton, Parametric study of development of inconel-steel functionally graded materials by laser direct metal deposition, *Materials & Design (1980-2015)* 54 (2014) 531–538.
- 900 [42] S. Liu, Y. C. Shin, Additive manufacturing of ti6al4v alloy: A review, *Materials & Design* 164 (2019) 107552.

- [43] F. Bartolomeu, M. Costa, N. Alves, G. Miranda, F. S. Silva, Selective laser melting of ti6al4v sub-millimetric cellular structures: Prediction of dimensional deviations and mechanical performance, *journal of the mechanical behavior of biomedical materials* 113 (2021) 104123.
- 905 [44] N. Shamsaei, A. Yadollahi, L. Bian, S. M. Thompson, An overview of direct laser deposition for additive manufacturing; part ii: Mechanical behavior, process parameter optimization and control, *Additive Manufacturing* 8 (2015) 12–35.
- 910 [45] S. Sing, S. Huang, G. Goh, G. Goh, C. Tey, J. Tan, W. Yeong, Emerging metallic systems for additive manufacturing: In-situ alloying and multi-metal processing in laser powder bed fusion, *Progress in Materials Science* 119 (2021) 100795.
- 915 [46] Z. Liu, D. Zhang, S. Sing, C. Chua, L. Loh, Interfacial characterization of slm parts in multi-material processing: Metallurgical diffusion between 316l stainless steel and c18400 copper alloy, *Materials Characterization* 94 (2014) 116–125. doi:<https://doi.org/10.1016/j.matchar.2014.05.001>.
URL <https://www.sciencedirect.com/science/article/pii/S1044580314001351>
- 920 [47] S. Sing, L. Lam, D. Zhang, Z. Liu, C. Chua, Interfacial characterization of slm parts in multi-material processing: Intermetallic phase formation between alsi10mg and c18400 copper alloy, *Materials Characterization* 107 (2015) 220–227.
- 925 [48] A. G. Demir, B. Previtali, Multi-material selective laser melting of fe/al-12si components, *Manufacturing letters* 11 (2017) 8–11.
- [49] P. Kumar, J. K. Santosa, E. Beck, S. Das, Direct-write deposition of fine powders through miniature hopper-nozzles for multi-material solid freeform fabrication, *Rapid Prototyping Journal* (2004) .

- [50] K. A. Mumtaz, N. Hopkinson, Laser melting functionally graded composition of waspaloy® and zirconia powders, *Journal of materials science* 42 (18) (2007) 7647–7656.
- [51] M. Ott, M. Zach, Multi-material processing in additive manufacturing, in: 2010 International Solid Freeform Fabrication Symposium, University of Texas at Austin, 2010.
- [52] Y. Chivel, New approach to multi-material processing in selective laser melting, *Physics Procedia* 83 (2016) 891–898.
- [53] C. Anstaett, C. Seidel, G. Reinhart, Fabrication of 3d multi-material parts using laser-based powder bed fusion, in: 2017 International Solid Freeform Fabrication Symposium, University of Texas at Austin, 2017.
- [54] Admatec, laserflux conflux, <https://admateceurope.com/#laserflex>, accessed: 2022-02-25.
- [55] J. Walker, J. R. Middendorf, C. C. Lesko, J. Gockel, Multi-material laser powder bed fusion additive manufacturing in 3-dimensions, *Manufacturing Letters* 31 (2022) 74–77.
- [56] W. Chiu, K. Yu, Direct digital manufacturing of three-dimensional functionally graded material objects, *Computer-Aided Design* 40 (12) (2008) 1080–1093.
- [57] R. Ponche, O. Kerbrat, P. Mognol, J.-Y. Hascoet, A novel methodology of design for additive manufacturing applied to additive laser manufacturing process, *Robotics and Computer-Integrated Manufacturing* 30 (4) (2014) 389–398.
- [58] W. Chiu, S. Tan, Multiple material objects: from cad representation to data format for rapid prototyping, *Computer-aided design* 32 (12) (2000) 707–717.

- 955 [59] Y. Siu, S. Tan, 'source-based' heterogeneous solid modeling, Computer-Aided Design 34 (1) (2002) 41–55.
- [60] T. R. Jackson, Analysis of functionally graded material object representation methods, Ph.D. thesis, Massachusetts Institute of Technology (2000).
- 960 [61] L. Patil, D. Dutta, A. D. Bhatt, K. Jurrens, K. Lyons, M. Pratt, R. D. Sriram, A proposed standards-based approach for representing heterogeneous objects for layered manufacturing, Rapid Prototyping Journal 8 (3) (2002) 134–146.
- [62] B. Bruegge, A. H. Dutoit, Object-Oriented Software Engineering Using UML, Patterns and Java-(Required), Vol. 2004, Prentice Hall, 2004.
- 965 [63] Slic3r - g-code generator for 3d printers, <http://slic3r.org/>, accessed: 2017-09-25.
- [64] Scalable Vector Graphics (SVG) 1.1. - second edition, <https://www.w3.org/TR/SVG/>, accessed: 2017-09-25.
- 970 [65] F. team, FreeCAD: 3D parametric modeler, <https://www.freecadweb.org/>, accessed: 2019-10-31 (2016).